Contents lists available at ScienceDirect

Physics Letters B

www.elsevier.com/locate/physletb

PHYSICS LETTERS B

2 TeV walking technirho at LHC?

CrossMark

Hidenori S. Fukano [a], Masafumi Kurachi [b], Shinya Matsuzaki [c,d,*], Koji Terashi [e], Koichi Yamawaki [a]

[a] *Kobayashi-Maskawa Institute for the Origin of Particles and the Universe (KMI), Nagoya University, Nagoya 464-8602, Japan*
[b] *Institute of Particle and Nuclear Studies, High Energy Accelerator Research Organization (KEK), Tsukuba 305-0801, Japan*
[c] *Institute for Advanced Research, Nagoya University, Nagoya 464-8602, Japan*
[d] *Department of Physics, Nagoya University, Nagoya 464-8602, Japan*
[e] *The University of Tokyo, International Center for Elementary Particle Physics and Department of Physics, 7-3-1 Hongo, Bunkyo-ku, JP - Tokyo 113-0033, Japan*

ARTICLE INFO

ABSTRACT

The ATLAS collaboration has recently reported an excess of about 2.5 σ global significance at around 2 TeV in the diboson channel with the boson-tagged fat dijets, which may imply a new resonance beyond the standard model. We provide a possible explanation of the excess as the isospin-triplet technivector mesons (technirhos, denoted as $\rho_\Pi^{\pm,3}$) of the walking technicolor in the case of the one-family model as a benchmark. As the effective theory for the walking technicolor at the scales relevant to the LHC experiment, we take a scale-invariant version of the hidden local symmetry model so constructed as to accommodate technipions, technivector mesons, and the technidilaton in such a way that the model respects spontaneously broken chiral and scale symmetries of the underlying walking technicolor. In particular, the technidilaton, a (pseudo) Nambu–Goldstone boson of the (approximate) scale symmetry predicted in the walking technicolor, has been shown to be successfully identified with the 125 GeV Higgs. Currently available LHC limits on those technihadrons are used to fix the couplings of technivector mesons to the standard-model fermions and weak gauge bosons. We find that the technirhos are mainly produced through the Drell–Yan process and predominantly decay to the dibosons, which accounts for the currently reported excess at around 2 TeV. The consistency with the electroweak precision test and other possible discovery channels of the 2 TeV technirhos are also addressed.

0. Introduction

The key particle responsible for the origin of the mass, a Higgs boson, was discovered at the LHC in 2012 [1]. However, the dynamical origin of the Higgs and hence of the electroweak (EW) symmetry breaking is yet to be elucidated, suggesting existence of a theory beyond the Standard Model (SM) to be explored at the LHC Run-II.

One of the candidates for the theory beyond the SM to account for the dynamical origin of the EW symmetry breaking is the walking technicolor based on the approximately scale-invariant gauge dynamics, which has a large anomalous dimension $\gamma_m \simeq 1$, and

the technidilaton, a pseudo Nambu–Goldstone (NG) boson of the approximate scale symmetry, as a light composite Higgs [2]. In this theory the EW symmetry breaking is triggered by the technifermion condensation $\langle \bar{F}F \rangle$, like the quark condensation $\langle \bar{q}q \rangle$ in QCD, and the technidilaton arises as a composite flavor-singlet scalar meson formed by the $\bar{F}F$-bound state, directly linking to the dynamical breaking mechanism of the EW symmetry. In a particular walking technicolor model, the "one-family model" with $N_F = 8$ technifermions, the technidilaton successfully accounts for the 125 GeV Higgs at LHC [3–7].

The one-family model, originally proposed as a naive scale-up version of QCD [8,9], in fact turned out to be a promising candidate for the walking technicolor in the new context of large N_F gauge theory with $SU(N_C)$ gauge group [10] through the conformal phase transition [11] characterized by the Miransky scaling which is the crucial ingredient of the walking technicolor [2]: the mass and the couplings of the technidilaton were calculated through both the

* Corresponding author.
E-mail addresses: fukano@kmi.nagoya-u.ac.jp (H.S. Fukano), kurachi@post.kek.jp (M. Kurachi), synya@hken.phys.nagoya-u.ac.jp (S. Matsuzaki), Koji.Terashi@cern.ch (K. Terashi), yamawaki@kmi.nagoya-u.ac.jp (K. Yamawaki).

ladder calculations and the holographic model, with the best fit to the 125 GeV Higgs for $N_F = 8$ and $N_C = 4$ [3–6].[1] Among other walking technicolor models, the one-family model is special in the sense that it is the most straightforward and natural model setting for the extended technicolor (ETC) as a standard way to give masses to the quarks and leptons. The value $N_C = 4$ is further selected as an interesting model setting within the ETC framework [13]. Furthermore, recent lattice studies [14–16] suggest that $N_F = 8$ QCD has desired walking signals of the condensate $\langle \bar{F}F \rangle$ with an approximate scale symmetry and a large anomalous dimension $\gamma_m \simeq 1$. Moreover, a light flavor-singlet scalar meson as a candidate for the technidilaton has been discovered on the lattice for the $N_F = 8$ QCD [17].[2]

Besides the technidilaton at 125 GeV, the one-family model of the walking technicolor predicts a rich composite spectra in several-TeV region to be seen at LHC Run II: the model consists of techniquarks (3-colored doublets) and technileptons (1-noncolored doublet), having the same SM quantum numbers as those of the one-generation of the SM fermions, and hence possesses a large global chiral symmetry, $SU(8)_L \times SU(8)_R$, in which the EW and QCD charges are partially embedded. The chiral symmetry as well as the EW symmetry is thus broken by the technifermion-chiral condensate, down to the vectorial symmetry $SU(8)_V$, giving rise to 63 NG bosons, the composite technipions, where 3 linear combinations of them are eaten by weak bosons W and Z, with the rest all becoming very massive to several-TeV scale by the explicit breaking of the $SU(8)_L \times SU(8)_R$ symmetry due to the ETC gauge interactions as well as the EW and the QCD gauge interactions.[3]

In addition, the walking technicolor has massive vector mesons (technirhos) which are suggested to have mass much heavier in units of the decay constant of technipion F_π than that of QCD rho mesons: $M_\rho / F_\pi \gg (M_\rho / F_\pi)_{\text{QCD}} \simeq 8$ in various calculations, ladder [22], holography [6] and the lattice [15,23]. The technirhos should couple to the weak boson pairs to be seen as distinct resonances in the diboson channel at the LHC. Discovering the technirhos in the diboson channel thus would be a smoking-gun of the walking technicolor. In particular, the one-family model predicts a rich spectra of 63 of such composite vector mesons at several-TeV scale, all of which will be discovered at Run II LHC.

Very recently, the ATLAS collaboration [24] has reported an excess of about 2.5 σ global significance at around 2 TeV in the diboson channel with the boson-tagged fat dijets. This may imply new resonance(s) like the technirhos.[4]

In this paper, we discuss possibilities to explain the excess from the one-family model of the walking technicolor which already successfully explained the 125 GeV Higgs in terms of the technidilaton. To address the technihadron phenomenologies at the LHC, we employ a low-energy effective theory for the walking technicolor, what we call the scale-invariant version of hidden local symmetry (sHLS) model [26], constructed from the low-lying technihadrons including the technidilaton, and technipions and technirhos. We constrain the couplings of the technirhos to the SM fermions and weak gauge bosons by taking into account currently available LHC limits on the technihadrons and the size of the resonance width $\lesssim 100$ GeV in the diboson channel with boson-tagged fat dijets implied by the ATLAS data [24].

We find that the isospin-triplet technirhos, denoted as $\rho_\Pi^{\pm,3}$, can have the couplings large enough to be mainly produced through the Drell–Yan (DY) process analogously to the ρ–γ mixing and predominantly decay into the dibosons. We then compute the fat-dijet mass distribution at almost the same level of the acceptance and efficiencies for the event selection as those in the ATLAS analysis [24], and find that the $\rho_\Pi^{\pm,3}$ with the mass of 2 TeV can account for the currently reported excess in the diboson channel. The consistency with the electroweak precision test and the discovery possibilities of the $\rho_\Pi^{\pm,3}$ in other channels are also discussed.

1. The model

We begin by introducing the effective technihadron Lagrangian (sHLS) for the one-family model of the walking technicolor [26], which is a version of the original HLS model [27] made scale-invariant so as to respect the scale symmetry of the underlying walking technicolor. The sHLS Lagrangian is constructed, based on the nonlinear realization of both the chiral $SU(8)_L \times SU(8)_R$ symmetry and the scale symmetry, together with the hidden local symmetry $[SU(8)_V]_{\text{HLS}}$, which is a spontaneously broken gauge symmetry. The model is characterized by the coset space $G/H = [SU(8)_L \times SU(8)_R \times [SU(8)_V]_{\text{HLS}}]/SU(8)_V$, with the basic quantities being the nonlinear bases ξ_L, ξ_R such that $\xi_L^\dagger \xi_R = e^{2i\pi/F_\pi}$ and $\chi(\phi) = e^{\phi/F_\phi}$. They are parametrized by the technipion fields (π) and the technidilaton (ϕ), with the technipion decay constant F_π and the technidilaton decay constant F_ϕ, respectively. In addition, ξ_L, ξ_R are also parameterized by the fictitious NG boson fields to be absorbed into the gauge bosons (technirhos) of the spontaneously broken HLS, V_μ, with the gauge coupling g. The practical building blocks are $\hat{\alpha}_{\perp\mu}$ and $\hat{\alpha}_{\parallel\mu}$, which are constructed from the G-nonlinear bases (ξ_L, ξ_R) as $\hat{\alpha}_{\parallel,\perp\mu} = (D_\mu \xi_R \xi_R^\dagger \pm D_\mu \xi_L \xi_L^\dagger)/2i$, where the covariant derivatives are $D_\mu \xi_L = \partial_\mu \xi_L - iV_\mu \xi_L + i\xi_L \mathcal{L}_\mu$ and $D_\mu \xi_R = \partial_\mu \xi_R - iV_\mu \xi_R + i\xi_R \mathcal{R}_\mu$ with the external gauge fields $(\mathcal{L}_\mu, \mathcal{R}_\mu)$ including the SM gauge fields. (More details such as the transformation properties of these nonlinear bases under the G-symmetry and scale symmetry are given in Ref. [26].)

The Lagrangian corresponding to the G- and scale-invariant action at the leading order of the derivative expansion is thus written as follows:

$$\mathcal{L} = F_\pi^2 \chi^2 \text{tr}[\hat{\alpha}_{\perp\mu}^2] + aF_\pi^2 \chi^2 \text{tr}[\hat{\alpha}_{\parallel\mu}^2] - \frac{1}{2g^2} \text{tr}[V_{\mu\nu}^2] + \frac{1}{2} F_\phi^2 (\partial_\mu \chi)^2 + \cdots, \quad (1)$$

where $V_{\mu\nu} = \partial_\mu V_\nu - \partial_\nu V_\mu - i[V_\mu, V_\nu]$ and a is a parameter to be fixed later. In Eq. (1) we have indicated, by the ellipsis, other terms explicitly breaking the G-symmetry and scale symmetry, including the ϕ-potential fixed by the scale anomaly of the underlying walking technicolor [4] and the SM gauge boson-kinetic terms. There

---

[1] In the ladder calculations, the light technidilaton can naturally be realized in the large N_C and N_F limit, with fixed $N_F/N_C (\gg 1)$ ("anti-Veneziano limit"), in a sense similar to the η' meson in QCD as a pseudo NG boson in the same limit, with $N_F/N_C (\ll 1)$ (Veneziano limit), both having the vanishing mass limit though not exact massless point. See discussions in Refs. [7,12]. The holographic model [6] gives even more reduction of the technidilaton mass due to the large technigluon condensate which is missing in the ladder approximation.

[2] A similar light flavor-singlet scalar meson on the lattice has also been found in the $N_F = 12$ QCD [18–20]. Although many lattice results indicate that the $N_F = 12$ is in the conformal window where the chiral and scale symmetries are not spontaneously broken and hence no dilaton exists, such a light scalar in $N_F = 12$ QCD may be a generic feature of the conformal (scale-symmetric) dynamics common to $N_F = 8$ QCD.

[3] Although there are only three exact NG bosons to be absorbed into W and Z, they are linear combinations of all the flavors and hence the system is completely different from the one-doublet model based on $SU(2)_L \times SU(2)_R/SU(2)_V$. Also note that the explicit breaking gauge interactions are rather weak at the relevant energy scale so that the masses of all the 60 left-over technipions may be estimated by the perturbative estimate, which are actually greatly enhanced to the several TeV's region by the large anomalous dimension of the walking dynamics. The discovery of the technipions at LHC Run II is an issue of the one-family model of the walking technicolor [21].

[4] The CMS has also done a similar diboson analysis and reported moderate excesses near 2 TeV [25].

are also higher derivative terms of $\mathcal{O}(p^4)$, etc., which will be discussed later.

The couplings of the technihadrons are obtained by expanding the sHLS Lagrangian in powers of the technihadron fields (π, ϕ, ρ_μ) embedded into $\xi_{L,R}, \chi$ and $V_\mu = g\rho_\mu$. The way of embedding technihadron fields and the SM gauge bosons into the 8-flavor matrix forms and the explicit expressions of the technihadron couplings (in the unitary gauge of the HLS) are given in Ref. [26]. Here we just pick up the couplings of the isospin-triplet color-singlet technirhos $(\rho_\Pi^\pm, \rho_\Pi^3)$ from the reference, which are relevant to the diboson resonance at the mass $M_{\rho_\Pi^\pm} = M_{\rho_\Pi^3} \equiv M_{\rho_\Pi} \simeq 2\,\text{TeV}.$[5]

The $\rho_\Pi^{\pm,3}$ couplings to the SM-f fermion pair arise from the mixing between the SM gauge bosons and $\rho_\Pi^{\pm,3}$ present in the (aF_π^2) term of Eq. (1) as an analogue of the ρ–γ mixing in QCD. The interaction terms take the form

$$\mathcal{L}_{\rho_\Pi ff} = -\sqrt{N_D}\frac{F_\rho}{M_{\rho_\Pi}}\left[eJ_\mu^{\text{em}}\rho_\Pi^{3\mu}\right.$$

$$+\frac{e(c^2-s^2)}{2sc}\frac{1}{1-m_Z^2/M_{\rho_\Pi}^2}J_\mu^Z\rho_\Pi^{3\mu}$$

$$\left.+\frac{e}{2s}\frac{1}{1-m_W^2/M_{\rho_\Pi}^2}(J_\mu^{W^+}\rho_\Pi^{+\mu}+\text{h.c.})\right], \quad (2)$$

where e and s $(c^2 = 1 - s^2)$ respectively denote the electromagnetic coupling and the (sine of) standard weak mixing angle. The SM fermion currents are defined as $J_\mu^{\text{em}} = e\sum_f \bar{f}\gamma_\mu Q_{\text{em}}^f f$, $J_\mu^Z = e/(sc)\sum_f\left[\bar{f}_L\gamma_\mu(\tau_3^f - s^2 Q_{\text{em}}^f)f_L + \bar{f}_R\gamma_\mu(-s^2 Q_{\text{em}}^f)f_R\right]$ and $J_\mu^{W^+} = e/(\sqrt{2}s)\sum_f \bar{f}_{uL}\gamma_\mu f_{dL}$ $(J_\mu^{W^-} = (J_\mu^{W^+})^\dagger)$ with the electromagnetic charge for the f-fermion Q_{em}^f and the isospin charges $\tau_3^f = \pm 1/2$ for the up- and down-sector $f_{u,d}$-fermions. The ρ_Π-SM gauge boson-mixing strength F_ρ is expressed in terms of the sHLS parameters as $F_\rho = \sqrt{a}F_\pi$. The prefactor $\sqrt{N_D}$ stands for the number of electroweak doublets formed by technifermions, which is 4 in the case of the one-family model. Note that the N_D dependence is canceled out in the combination $(\sqrt{N_D}F_\rho)$: $\sqrt{N_D}F_\rho = \sqrt{N_D}\sqrt{a}F_\pi = \sqrt{a}v_{\text{EW}}$ where $v_{\text{EW}} \simeq 246\,\text{GeV}$ (see also Eq. (7) below). In reaching Eq. (2) we have also used the ρ_Π mass formula obtained from the (aF_π^2) term of Eq. (1):

$$M_{\rho_\Pi} = \sqrt{a}gF_\pi = 2\,\text{TeV}, \quad (3)$$

where we have set it to 2 TeV for the present analysis.

As to the couplings to the weak gauge bosons, the ρ_Π mainly couples to the longitudinal modes $(W_\mu, Z_\mu)_L = (\partial_\mu\pi_W/m_W, \partial_\mu\pi_Z/m_Z)$,[6] where π_W and π_Z stand for the NG bosons eaten by the W and Z, respectively. The ρ_Π–W_L–W_L/Z_L vertices thus arise from the (aF_π^2) term of Eq. (1):

$$\mathcal{L}_{\rho_\Pi W_L W_L/W_L Z_L} = \frac{1}{\sqrt{N_D}}g_{\rho\pi\pi}i\Big[\partial^\mu\pi_W^+\pi_W^-\rho_{\Pi\mu}^3$$

$$+(\partial^\mu\pi_W^-\pi_Z-\partial^\mu\pi_Z\pi_W^-)\rho_{\Pi\mu}^+\Big]+\text{h.c.}, \quad (4)$$

where $g_{\rho\pi\pi} = (1/2)ag$ in terms of the original Lagrangian parameters. Note the prefactor $(1/\sqrt{N_D})$ in front of the ρ–π–π coupling: this is the characteristic feature of the one-family model of walking technicolor and realizes the smaller $\rho \to W_L W_L$ width by a factor of $(1/N_D) = 1/4$, compared to the naive scale-up version of QCD having only the one weak doublet, as will be seen clearly below.

It turns out that the ρ_Π does not couple to the technidilaton ϕ involving the SM gauge bosons (W, Z and photon γ) because of the scale invariance [28].

As we mentioned before, all the 60 technipions not eaten by the W and Z bosons in the one-family model acquire masses due to the explicit breaking of the $SU(8)_L \times SU(8)_R$ chiral symmetry by the EW and QCD as well as the ETC gauge couplings, which are enormously enhanced to the order of $\mathcal{O}(\text{a few TeV})$ by the large anomalous dimension $\gamma_m \simeq 1$ as a salient feature of the walking technicolor [21], and hence should be larger than the technirho mass. Thereby, we will ignore the 2 TeV ρ_Π couplings to technipions.

In addition to the leading order terms in Eq. (1), one may incorporate higher-derivative coupling terms, so-called $\mathcal{O}(p^4)$ terms, introduced as in the original HLS formulation applied to QCD [29, 30],

$$\mathcal{L}' = z_3\text{tr}[\hat{\mathcal{V}}_{\mu\nu}V^{\mu\nu}] + iz_4\text{tr}[V^{\mu\nu}\hat{\alpha}_{\perp\mu}\hat{\alpha}_{\perp\nu}], \quad (5)$$

where $\hat{\mathcal{V}}_{\mu\nu}$ becomes $1/2[\partial_\mu(\mathcal{R}_\nu + \mathcal{L}_\nu) - \partial_\nu(\mathcal{R}_\mu + \mathcal{L}_\mu)] +$ (non-Abelian terms and technipion terms) in the unitary gauge of the HLS. The order of magnitude for the parameters z_3 and z_4 can be estimated by the naive dimensional analysis to be $z_{3,4} = \mathcal{O}(N_C/(4\pi)^2) = \mathcal{O}(10^{-2})$ for $N_C = 4$. These terms affect the ρ_Π–f–f and ρ_Π–W_L–W_L/Z_L couplings at the on-shell of the ρ_Π: the F_ρ coupling in Eq. (2) and the $g_{\rho\pi\pi}$ coupling in Eq. (4) are then modified as

$$F_\rho = \sqrt{a}F_\pi \to F_\rho = \sqrt{a}F_\pi(1-g^2z_3),$$
$$g_{\rho\pi\pi} = \frac{1}{2}ag \to g_{\rho\pi\pi} = \frac{1}{2}ag(1-\frac{1}{2}g^2z_4). \quad (6)$$

Thus, by including the possible higher derivative terms, the couplings relevant to the 2 TeV ρ_Π phenomenology are found to be controlled by the four parameters F_π, g, z_3 and z_4 with the parameters a and F_ϕ being redundant for the present analysis. In place of the original parameters z_3 and z_4, we shall use F_ρ and $g_{\rho\pi\pi}$ with the replacement in Eq. (6) taken into account. Among those four parameters, the technipion decay constant F_π is related to the EW scale $v_{\text{EW}} \simeq 246\,\text{GeV}$ for the one-family model with four weak-doublets, $N_D = N_F/2 = 4$, as

$$F_\pi = v_{\text{EW}}/\sqrt{N_D} \simeq 123\,\text{GeV}, \quad (7)$$

through the W/Z mass formula obtained by examining the F_π^2 term in Eq. (1). The HLS gauge coupling g is then determined through the ρ_Π mass formula in Eq. (3), once the ρ_Π mass is set to 2 TeV and the parameter a is chosen. Then, with two inputs (F_π, M_{ρ_Π}), we are left only with the two parameters

$$(F_\pi, g, z_3, z_4) \longrightarrow (F_\rho, g_{\rho\pi\pi}), \quad (8)$$

which control the ρ_Π couplings to the SM fermions (Eq. (2)) and the weak gauge bosons (Eq. (4)), respectively.

---

[5] The Lagrangian Eq. (1) contains other isospin-triplet color-singlet technirhos $\rho_P^{\pm,3}$ which are not produced by the Drell–Yan process by the $SU(8)$ symmetry [26]. Although the $SU(8)_V$ symmetry as well as the full chiral symmetry $SU(8)_L \times SU(8)_R$ is already violated explicitly in Eq. (1) due to the introduction of the SM gauge couplings, there still exist no mixings between the ρ_Π^i and ρ_P^i at tree level, as explicitly shown in Ref. [26]. They do not mix at one-loop level $\mathcal{O}(p^4)$, neither. They can actually mix each other through the electroweak interactions at two-loop order $\mathcal{O}(p^6)$, which are highly suppressed by the loop factor to be negligible for the discussions in the present case.

[6] The ρ_Π couplings to the transverse modes of the weak gauge bosons turn out to be highly suppressed by a factor of $(m_{W/Z}/M_{\rho_\Pi})^2$, hence the ρ_Π are hardly produced via the vector boson fusion and vector–boson associate processes [28].
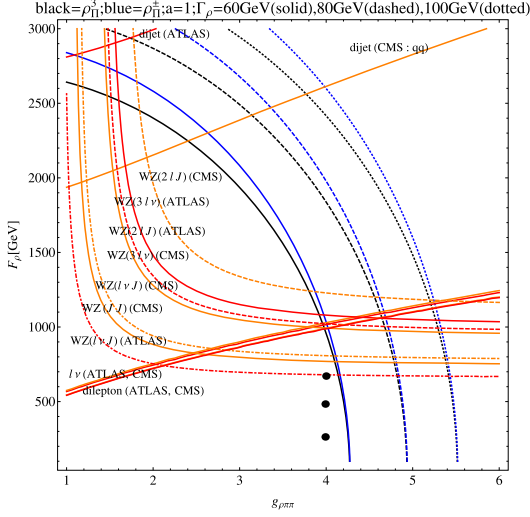
Fig. 1. The contours in the $(g_{\rho\pi\pi}, F_\rho)$ plane drawn by requiring the total widths $\Gamma_{\rho_\Pi^3}$ (black curves, in the right-middle) or $\Gamma_{\rho_\Pi^\pm}$ (blue curves, in the left-middle) to be 60 (solid), 80 (dashed), 100 (dotted) GeV at the mass of 2 TeV. The 95% C.L. upper limits at around 2 TeV from the LHC experiments [25,34–43] have also been shown together. The regions above those curves are excluded. The there black blobs denote the reference points in Eq. (11) with Eq. (10). (For interpretation of the references to color in this figure legend, the reader is referred to the web version of this article.)

2. Constraining the ρ_Π couplings

Using Eqs. (2), (4) we compute the partial decay widths of the $\rho_\Pi^{\pm,3}$ as functions of F_ρ and $g_{\rho\pi\pi}$. The $\rho_\Pi^{\pm,3}$ couplings are implemented by using the FeynRules [31] and the MadGraph5_aMC@NLO [32] is used for the estimation of the decay widths. We constrain the size of the total widths to be $\lesssim 100$ GeV in light of the ATLAS data on the diboson-tagged dijet mass distribution [24], so that the relevant couplings F_ρ and $g_{\rho\pi\pi}$ are constrained.

In Fig. 1 we show the contour plot in the $(F_\rho, g_{\rho\pi\pi})$ plane together with the 95% C.L. limits at around 2 TeV for W'/Z' candidates reported from the ATLAS and CMS experiments [25,33–43].[7] The upper bounds of the cross sections used to make the plots are as follows:

$$\sigma^{\mathrm{ATLAS}}_{WZ(3l\nu)}[\mathrm{fb}] \leq 22, \qquad \sigma^{\mathrm{CMS}}_{WZ(3l\nu)}[\mathrm{fb}] \leq 19,$$
$$\sigma^{\mathrm{ATLAS}}_{WZ(2lJ)}[\mathrm{fb}] \leq 20, \qquad \sigma^{\mathrm{CMS}}_{WZ(2lJ)}[\mathrm{fb}] \leq 27,$$
$$\sigma^{\mathrm{ATLAS}}_{WZ(l\nu J)}[\mathrm{fb}] \leq 9.5, \qquad \sigma^{\mathrm{CMS}}_{WZ(l\nu J)}[\mathrm{fb}] \leq 13$$
$$\sigma^{\mathrm{CMS}}_{WZ(JJ)}[\mathrm{fb}] \leq 12,$$
$$\sigma^{\mathrm{ATLAS}}_{l\nu}[\mathrm{fb}] \leq 0.41, \qquad \sigma^{\mathrm{CMS}}_{l\nu}[\mathrm{fb}] \leq 0.42$$
$$\sigma^{\mathrm{ATLAS}}_{2l}[\mathrm{fb}] \leq 0.24, \qquad \sigma^{\mathrm{CMS}}_{2l}[\mathrm{fb}] \leq 0.25$$
$$\sigma^{\mathrm{ATLAS}}_{2j}[\mathrm{fb}] \leq 130, \qquad \sigma^{\mathrm{CMS}}_{2j(qq)}[\mathrm{fb}] \leq 58, \qquad (9)$$

where in the last line we have quoted the upper limit set on generic narrow resonances (with the width being 0.1 percent of the mass) decaying to the qq-jet reported from the CMS

group [34], while the ATLAS bound [33] includes all the jet candidates. The ρ_Π cross sections have been computed by using CTEQ6L1 [46] parton distribution functions. Though the result is not changed by the value of the parameter a,[8] for just a practical reason, we have chosen $a = 1$ in computing the cross sections and decay widths. From the figure, we see that the $g_{\rho\pi\pi}$ coupling is constrained by requiring the total width for $\rho_\Pi^\pm$ to be $\Gamma_{\rho_\Pi^\pm} \lesssim 100$ GeV as $g_{\rho\pi\pi} \lesssim 5.5$. Hereafter, as a reference value, we shall take[9]

$$g_{\rho\pi\pi} = 4. \qquad (10)$$

As to the F_ρ, we may choose a typical set of the values satisfying the current LHC limits as

$$F_\rho[\mathrm{GeV}] = 250, 500, 650, \qquad (11)$$

in which the first value (250 GeV) is supported from nonperturbative calculations of a large N_F walking gauge theory [15,22], which are currently possible to quote at hand, the third one (650 GeV) is a representative of the maximal value satisfying the dilepton constraint, and the middle value (500 GeV) is just a sample in between the other two.[10]

For the values in Eqs. (10) and (11), we have the total widths,

$$\Gamma_{\rho_\Pi^3}[\mathrm{GeV}] \simeq (53, 55, 56),$$
$$\Gamma_{\rho_\Pi^\pm}[\mathrm{GeV}] \simeq (53, 54, 55),$$
$$\text{for } F_\rho[\mathrm{GeV}] = (250, 500, 650), \qquad (12)$$

and the dominant branching ratios,

$$\mathrm{Br}(\rho_\Pi^3 \to WW)[\%] \simeq (99, 96, 94),$$
$$\mathrm{Br}(\rho_\Pi^\pm \to W^\pm Z)[\%] \simeq (99, 97, 95),$$
$$\text{for } F_\rho[\mathrm{GeV}] = (250, 500, 650). \qquad (13)$$

The $\rho_\Pi^{\pm,3}$ are mainly produced via the DY process with the F_ρ as in Eq. (11). The total cross sections $\sigma_{\mathrm{DY}}(pp \to \rho_\Pi^{\pm,3})$ at the center of mass energy $\sqrt{s} = 8$ TeV are computed by using the CTEQ6L1 [46] parton distribution functions to be

$$\sigma_{\mathrm{DY}}(pp \to \rho_\Pi^3)[\mathrm{fb}] \simeq (0.7, 2.8, 4.7),$$
$$\sigma_{\mathrm{DY}}(pp \to \rho_\Pi^\pm)[\mathrm{fb}] \simeq (1.4, 5.4, 9.3),$$
$$\text{for } F_\rho[\mathrm{GeV}] = (250, 500, 650). \qquad (14)$$

Other subdominant decay and production properties are to be given in another publication [28].

---

[7] In addition to limits shown in Fig. 1, there are other limits from $W'/Z' \to$ Higgs plus weak bosons reported from the ATLAS and CMS [44,45], in which the analyses are based on the Higgs decay to bb or WW. However, the ρ_Πs in the present study do not decay to the Higgs candidate (technidilaton) [28], so we have not incorporated those constraints in the figure.

[8] The parameter choice $a = 1$ is special, corresponding to the locality of the deconstructed extra dimension (3-site model in the linear moose).

[9] The $g_{\rho\pi\pi}$ is slightly smaller than the QCD value $\simeq 6$ for $N_C = 3$, which can be understood by the N_C scaling, $g_{\rho\pi\pi}|_{N_C=4} \sim \sqrt{3/N_C} g_{\rho\pi\pi}|_{N_C=3}$ and destructive axialvector-a_1 contribution which is mimicked by the size of z_4 in the sHLS model (see also summary and discussion in the later section).

[10] In terms of the original Lagrangian parameters, g, z_3 and z_4 in Eqs. (1), (5) and (6), we have $g \simeq 16$, $z_4 \simeq 4.0 \times 10^{-3}$ and $z_3 \simeq (-4.0, -12, -18) \times 10^{-3}$ for $a = 1$, $g_{\rho\pi\pi} = 4$, $M_{\rho_\Pi} = 2$ TeV and $F_\rho = (250, 500, 650)$ GeV. The estimated size of z_3 and z_4 are compatible with the order of magnitude estimated by the naive dimensional analysis, $\mathcal{O}(N_C/(4\pi)^2)$ (see also text). The large value of g implies large corrections from higher order in the HLS chiral perturbation theory, with the expansion parameter $\xi = N_F \cdot g^2/(4\pi)^2 \simeq N_F \cdot p^2/(4\pi F_\pi)^2|_{p=M_\rho} \simeq 16 \gg 1$ ($N_F = 8$), in comparison with the real-life QCD ($N_F = 3$), $\xi \simeq 1$. Origin of the large corrections will be discussed in the Summary and discussion.

3. The technirho signals at 2 TeV in the fat-dijet mass distribution with the diboson-tagged

Now that all the parameters are fixed, we are ready to discuss the ρ_Π signals in the dijet mass distribution with the EW diboson tagged, in comparison with the ATLAS data [24]. To calculate the dijet mass distribution, we use the `FeynRules` [31] to implement the ρ_Π couplings, fixed as above, into the `Mad-Graph5_aMC@NLO` [32] and generate the cross sections at the parton level. For the hadronization and parton showering, `PYTHIA 8.1.86` [47] is used. The events are generated by using the `CTEQ6L1` [46] parton distribution functions and the jets are reconstructed through the Cambridge–Aachen algorithm [48,49] with the radius parameter $R = 1.2$ (C/A $R = 1.2$) by the `FastJet 3.0.6` [50].

To make a direct comparison with the ATLAS analysis, the C/A $R = 1.2$ jets (called fat-jets hereafter) are processed through a splitting and filtering algorithm described as "BDRS-A" in Ref. [51], similar to the algorithm in Ref. [52] but modified for high-p_T boson jets in ATLAS analysis. After that, we apply the same event selections as in Ref. [24]: i) the number of fat-jets ≥ 2; ii) the momentum balance $\sqrt{y_f} = \min(p_T^{j1}, p_T^{j2})\Delta R_{12}/m_{12} \geq 0.45$, where p_T^{j1} and p_T^{j2} are the transverse momenta of the two leading subjets found by the BDRS-A algorithm, ΔR_{12} and m_{12} are the η–ϕ distance and mass of the two subjets, respectively; iii) the transverse momentum p_T for the leading fat-jet J_1, $p_T(J_1) \geq 540$ GeV; iv) the pseudo-rapidity η for the two leading fat-jets $J_{1,2}$, $|\eta(J_1, J_2)| \leq 2$; v) the rapidity difference Δy between the two leading fat-jets, $\Delta y = |y(J_1) - y(J_2)| \leq 1.2$; vi) the p_T asymmetry for the two leading fat-jets, $\frac{p_T(J_1) - p_T(J_2)}{p_T(J_1) + p_T(J_2)} \leq 0.15$; vii) the number of charged-particle tracks associated with the original ungroomed fat-jet, $n_{\mathrm{tr}} < 30$; viii) the range of the fat-jet masses, M_{J_1, J_2}, $82.4 - 13 \leq M_{J_1, J_2}$ [GeV] $\leq 82.4 + 13$ for the WW selection, $92.8 - 13 \leq M_{J_1, J_2}$ [GeV] $\leq 92.8 + 13$ for the ZZ selection, and $92.8 - 13 \leq M_{J_1}$ [GeV] $\leq 92.8 + 13$, $82.4 - 13 \leq M_{J_2}$ [GeV] $\leq 82.4 + 13$, for the WZ selection where $M_{J_1} > M_{J_2}$. For vii), since the charged-particle track reconstruction is not performed in this study, the n_{tr} requirement is not directly applied. Instead, assuming that the $\rho_\Pi^{\pm,3}$ has the same n_{tr} distribution as the W' signal used in ATLAS (Fig. 1b of Ref. [24]) and hence the scaling factor $(0.90 \pm 0.08$ in Ref. [24]) defined as the ratio of the n_{tr} cut efficiency in data to that in the W' simulation is applicable, the $\rho_\Pi^{\pm,3}$ signal yields are scaled by the square of the product of the cut efficiency and the scaling factor. The cut efficiency is estimated from the W' signal distribution shown in Fig. 1b of Ref. [24]. In addition, to account for the migration due to ATLAS detector resolution, the fat-jet momentum/energy and mass values are smeared by Gaussian distributions with the mean of 0 and the standard deviations of 5% (as in Ref. [24]) and 8% (taken from $600 < p_T < 1000$ GeV bin in Table 2 of Ref. [51]), respectively.

In Fig. 2 we show the technirho ρ_Π signals in the fat-dijet mass distributions with the diboson tagged for the WW (top panel) and WZ (bottom panel) selections at $\sqrt{s} = 8$ TeV and the integrated luminosity $\mathcal{L} = 20.3$ fb^{-1}. From the ATLAS result [24] we see that at 2.0 (1.9) TeV, the number of observed events are 8(5) and 7(4) per 100 GeV bin over the expected background $\simeq 2$ (3) for the WZ and WW selections, respectively. In comparison with the data, Fig. 2 implies that the 2 TeV $\rho_\Pi^{\pm,3}$ with $F_\rho = 650$ GeV can explain the excess with about 3 σ local (2.5 σ global) significance for both the WW and WZ selections.

The ATLAS collaboration [24] has also reported an excess by about 2.9 σ (local significance) in the ZZ channel. As listed in the item viii) of the event selection above, the WW, WZ and ZZ selections are distinguished only by the fat-jet mass ranges,
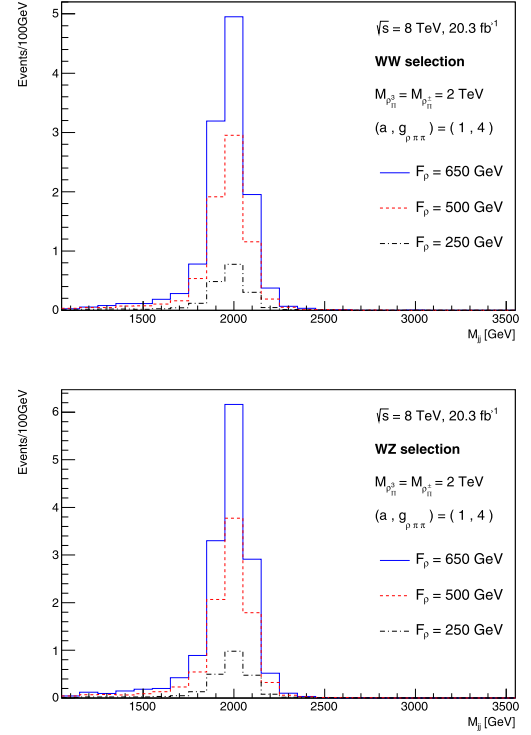

Fig. 2. The fat-dijet mass distribution M_{JJ} of $\rho_\Pi^{\pm,3}$ for the WW (top panel) and the WZ (bottom panel) selections at 2 TeV with F_ρ[GeV] $= 250$ (dashed–dotted line), 500 (dashed line), 650 (solid line).

hence the Z boson (e.g. its charge) is not clearly identified in the analysis. Therefore, the $\rho_\Pi \to WW/WZ$ events may contaminate in the ZZ channel, although the ρ_Π does not couple to ZZ in the model discussed here. In Fig. 3 we plot the fat-jet mass distributions of the 2 TeV $\rho_\Pi^{\pm,3}$ in the ZZ selection for F_ρ[GeV] $= 250, 500, 650$. From the ATLAS result [24] we read off the 3 (5) observed events/100 GeV over the expected background $\simeq 0.6(0.9)$ at 2.0 (1.9) TeV. The figure shows that the 2 TeV $\rho_\Pi^{\pm,3}$ with $F_\rho = 650$ GeV can also account for the excess in the ZZ channel.

4. Summary and discussion

In summary, we have discussed the 2 TeV diboson signals for the isospin-triplet color-singlet technirhos ($\rho_\Pi^{\pm,3}$) in the one-family model of the walking technicolor. It has been shown that the $\rho_\Pi^{\pm,3}$ with the narrow width $\lesssim 100$ GeV and a large Drell–Yan coupling, such as $F_\rho/M_{\rho_\Pi}(= 650\,\mathrm{GeV}/2000\,\mathrm{GeV}) \simeq 0.3$, can account for the excesses in the fat-dijet mass distributions in the diboson channel recently reported from the ATLAS group, consistently with the current-observed limits in other channels.

Some comments are in order:

1) We have shown in Fig. 3 that the 2 TeV $\rho_\Pi^{\pm,3}$ with $F_\rho = 650$ GeV is consistent with the excess seen in the ZZ channel. This is largely because the $\rho_\Pi \to WW/WZ$ events become broadly distributed in fat-jet mass due to finite detector resolution and hence some fraction of events are selected by the fat-jet mass cut of the ZZ selection. The experimental capability to separate WW/WZ from ZZ in decays of high-mass resonances will be an important ingredient to further test the models discussed in this study. Exploiting the leptonic ZZ decays ($\ell\ell q\bar{q}$, $\ell\ell\ell'\ell'$) will provide a handle to separate them from WW or WZ decay, while it requires a large dataset due to a small $Z \to \ell\ell$ branching fraction. Hence it is in-
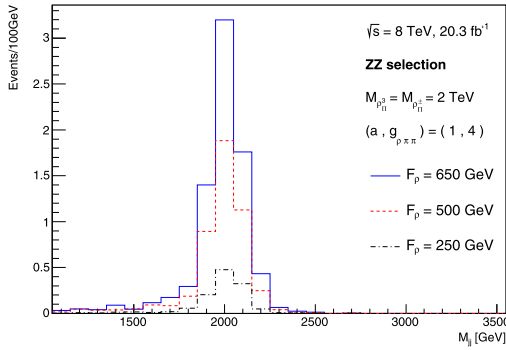
Fig. 3. The fat-dijet mass distribution M_{JJ} of $\rho_\Pi^{\pm,3}$ for the ZZ selection at 2 TeV with $F_\rho[\text{GeV}] = 250$ (dashed–dotted line), 500 (dashed line), 650 (solid line).

teresting to explore separation techniques based on the hadronic W/Z decays.

Shown in Fig. 1 of Ref. [24] are reconstructed fat-jet mass distributions of hadronically decaying W and Z bosons, as simulated for the 1.8 TeV graviton decaying into WW/ZZ. As clearly seen, the W and Z bosons can be statistically separated by ~ 10 GeV at peak positions if the excess remains and sufficient statistics is accumulated. In addition, the ATLAS study on charged-particle tracks associated with fat-jets from high-p_T hadronic $W^\pm$ bosons Ref. [53] shows that the W^+ and W^- can be separated at the level of $\sim 50\%$ W^+ efficiency with W^- rejection of about 4. This technique is expected to be less performant for separation between WW and ZZ resonances because a mixture of $W^\pm$ in WW would be less distinguishable from Z in ZZ on average. We however expect this charge measurement to provide additional discrimination between WZ and ZZ resonances by adopting the technique separately to higher and lower mass fat-jets in selected events.

2) The sHLS model we have employed throughout the present study can be viewed as the low-energy effective theory induced from the underlying walking technicolor. Actually, the DY coupling of the technirho, (F_ρ/M_ρ), detected at the LHC, should include contributions from not only the walking technicolor sector, but also an ETC sector, which communicates between the technifermion and the SM fermion sectors and hence necessary to account for the SM-fermion mass generation. The ETC yields an effective four-fermion interaction among the technifermions of the form $(\bar{F}\gamma_\mu T_a F)^2$, with T_a being the $SU(N_F)$ generators, which affects F_ρ. In that sense, the size of the F_ρ constrained by the current LHC data, mainly from the dilepton channel, would imply the desired amount of the ETC contributions: one may take the value of the DY coupling estimated only from the walking technicolor sector to be $F_\rho^{TC} \simeq 250$ GeV, supported from the result of nonperturbative calculations presently at hand [15,22]. Then the rest may be supplied from the ETC, say $F_\rho^{ETC}[\text{GeV}] = (0, 250, 400)$ for the total $F_\rho[\text{GeV}] = (F_\rho^{TC} + F_\rho^{ETC})[\text{GeV}] = (250, 500, 650)$. This implies an indirect constraint on modeling of the ETC derived from the current LHC data from the dilepton channel. Note that in the present analysis, such ETC effects can be, in a sense, mimicked by the parameter z_3 in Eq. (5) which shifts the F_ρ as in Eq. (6) just like $F_\rho \to F_\rho = F_\rho^{TC} + F_\rho^{ETC}$.

3) With such a large DY coupling of the technirho at hand, one might suspect the large contribution to the S parameter [54]. One can in fact estimate the size of the S coming only from the technirho contribution within the sHLS model, to find $S|_\rho = 4\pi N_D (F_\rho/M_{\rho_\Pi})^2 \simeq \mathcal{O}(10)$ for $F_\rho = 650$ GeV, where $N_D = 4$ for the one-family model. However, the techni-axialvector (techni-a_1) contribution may cancel the large $S|_\rho$ term: in the one-family model of the walking technicolor, it has been suggested from

several approaches [6,15,22,55] that the masses of the techni-ρ and -a_1 mesons are degenerate, $M_{\rho_\Pi} \simeq M_{a_{1\Pi}}$, due to the characteristic walking feature. Taking into account this, one may add the techni-a_1 meson contribution to the S as $S = S|_\rho + S|_{a_1} = 4\pi N_D (F_\rho/M_{\rho_\Pi})^2 [1 - (F_{a_1}/F_\rho)^2]$. Thus, if $F_{a_1} \simeq F_\rho$ (including possible ETC contributions), the S parameter can be vanishingly small to be $\simeq 0$, as it happens in a different context [56]: this can actually take place in the one-family model of the walking technicolor, in view of a holographic dual [57]. If it is the case we may expect a new type DY process through the techni-a_1 meson at 2 TeV.

4) Note also that the presence of the techni-a_1 mesons generically modify the $g_{\rho\pi\pi}$ coupling due to the mixing between the pions and axialvector mesons, as in the case of the generalized HLS model [58] in application to QCD. Such a role of the shift effects can actually be played by the z_4 term in Eq. (5), instead of the techni-a_1 mesons, as in Eq. (6).

5) As to the DY coupling, it is furthermore indicated that if the diboson excess is explained by the presence of the 2 TeV technirhos $\rho_\Pi^{\pm,3}$ with the large DY coupling $F_\rho = 650$ GeV which barely satisfies the current dilepton limit, the 2 TeV $\rho_\Pi^{\pm,3}$, as well as the 2 TeV techni-a_1 mesons having the same amount of the DY coupling F_{a_1} to suppress the S parameter, can necessarily be seen also in the dilepton channel as quite narrow resonances at the LHC-Run II, which could be possible at the earlier stage of the running. To put it the other way around, if the ρ_Π and techni-a_1 would have somewhat small DY coupling like $F_\rho = 250$ GeV or less and the diboson excess goes away in the future, it might be hard to detect the ρ_Π and techni-a_1 at the LHC. Other technirhos in the one-family model could then be discovered through other channels. In this sense, the fate of the currently reported diboson excess is linked with which channels and technivectors and techni-axialvectors are accessible at the LHC-Run II.

More detailed analysis on the promising LHC signals for the technivector and axialvector mesons in the one-family model of the walking technicolor will be pursued in the future [28].

References

[1] G. Aad, et al., ATLAS Collaboration, Phys. Lett. B 716 (2012) 1;
    S. Chatrchyan, et al., CMS Collaboration, Phys. Lett. B 716 (2012) 30.
[2] K. Yamawaki, M. Bando, K. Matumoto, Phys. Rev. Lett. 56 (1986) 1335;
    M. Bando, K. Matumoto, K. Yamawaki, Phys. Lett. B 178 (1986) 308.
[3] S. Matsuzaki, K. Yamawaki, Phys. Rev. D 85 (2012) 095020.
[4] S. Matsuzaki, K. Yamawaki, Phys. Rev. D 86 (2012) 035025.
[5] S. Matsuzaki, K. Yamawaki, Phys. Lett. B 719 (2013) 378;
    S. Matsuzaki, arXiv:1304.4882 [hep-ph].
[6] S. Matsuzaki, K. Yamawaki, Phys. Rev. D 86 (2012) 115004.
[7] S. Matsuzaki, Talk given at the Sakata Memorial KMI Workshop on "Origin of mass and strong coupling gauge theories" (SCGT15), KMI, Nagoya University, 2015, http://www.kmi.nagoya-u.ac.jp/workshop/SCGT15/.
[8] E. Farhi, L. Susskind, Phys. Rev. D 20 (1979) 3404;
    S. Dimopoulos, Nucl. Phys. B 168 (1980) 69.
[9] For a review see E. Farhi, L. Susskind, Phys. Rep. 74 (1981) 277.
[10] T. Appelquist, J. Terning, L.C.R. Wijewardhana, Phys. Rev. Lett. 77 (1996) 1214.
[11] V.A. Miransky, K. Yamawaki, Phys. Rev. D 55 (1997) 5051;
    V.A. Miransky, K. Yamawaki, Phys. Rev. D 56 (1997) 3768.
[12] M. Kurachi, S. Matsuzaki, R. Shrock, K. Yamawaki, in preparation.
[13] M. Kurachi, R. Shrock, K. Yamawaki, Phys. Rev. D 91 (5) (2015) 055032.
[14] Y. Aoki, T. Aoyama, M. Kurachi, T. Maskawa, K.-i. Nagai, H. Ohki, A. Shibata, K. Yamawaki, T. Yamazaki, the LatKMI Collaboration, Phys. Rev. D 87 (2013) 094511.
[15] T. Appelquist, et al., LSD Collaboration, Phys. Rev. D 90 (11) (2014) 114502.

[16] A. Hasenfratz, D. Schaich, A. Veernala, arXiv:1410.5886 [hep-lat].
[17] Y. Aoki, T. Aoyama, M. Kurachi, T. Maskawa, K. Miura, K.-i. Nagai, H. Ohki, E. Rinaldi, A. Shibata, K. Yamawaki, T. Yamazaki, the LatKMI Collaboration, Phys. Rev. D 89 (2014) 111502(R);
Y. Aoki, T. Aoyama, M. Kurachi, T. Maskawa, K. Miura, K.-i. Nagai, H. Ohki, E. Rinaldi, A. Shibata, K. Yamawaki, T. Yamazaki, the LatKMI Collaboration, PoS LATTICE 2013 (2013) 070.
[18] Y. Aoki, T. Aoyama, M. Kurachi, T. Maskawa, K.-i. Nagai, H. Ohki, E. Rinaldi, A. Shibata, K. Yamawaki, T. Yamazaki, the LatKMI Collaboration, Phys. Rev. Lett. 111 (16) (2013) 162001.
[19] Z. Fodor, K. Holland, J. Kuti, D. Nogradi, C.H. Wong, PoS LATTICE 2013 (2014) 062.
[20] R. Brower, A. Hasenfratz, C. Rebbi, E. Weinberg, O. Witzel, PoS LATTICE 2014 (2014) 254.
[21] M. Kurachi, S. Matsuzaki, K. Yamawaki, Phys. Rev. D 90 (9) (2014) 095013;
J. Jia, S. Matsuzaki, K. Yamawaki, Phys. Rev. D 87 (1) (2013) 016006.
[22] M. Harada, M. Kurachi, K. Yamawaki, Phys. Rev. D 68 (2003) 076001.
[23] Y. Aoki, T. Aoyama, E. Bennett, M. Kurachi, T. Maskawa, K. Miura, K.-i. Nagai, H. Ohki, E. Rinaldi, A. Shibata, K. Yamawaki, T. Yamazaki, the LatKMI Collaboration, in preparation;
Y. Aoki, LatKMI Collaboration, Talk given at the Sakata Memorial KMI Workshop on "Origin of mass and strong coupling gauge theories" (SCGT15), KMI, Nagoya University, 2015, http://www.kmi.nagoya-u.ac.jp/workshop/SCGT15/.
[24] G. Aad, et al., ATLAS Collaboration, arXiv:1506.00962 [hep-ex].
[25] V. Khachatryan, et al., CMS Collaboration, J. High Energy Phys. 1408 (2014) 173.
[26] M. Kurachi, S. Matsuzaki, K. Yamawaki, Phys. Rev. D 90 (5) (2014) 055028.
[27] M. Bando, T. Kugo, S. Uehara, K. Yamawaki, T. Yanagida, Phys. Rev. Lett. 54 (1985) 1215;
M. Bando, T. Kugo, K. Yamawaki, Nucl. Phys. B 259 (1985) 493;
M. Bando, T. Fujiwara, K. Yamawaki, Prog. Theor. Phys. 79 (1988) 1140;
M. Bando, T. Kugo, K. Yamawaki, Phys. Rep. 164 (1988) 217–314.
[28] H.S. Fukano, M. Kurachi, S. Matsuzaki, K. Terashi, K. Yamawaki, in preparation.
[29] M. Tanabashi, Phys. Lett. B 316 (1993) 534.
[30] For a review, see M. Harada, K. Yamawaki, Phys. Rep. 381 (2003) 1.
[31] N.D. Christensen, C. Duhr, Comput. Phys. Commun. 180 (2009) 1614;
A. Alloul, N.D. Christensen, C. Degrande, C. Duhr, B. Fuks, Comput. Phys. Commun. 185 (2014) 2250.
[32] J. Alwall, R. Frederix, S. Frixione, V. Hirschi, F. Maltoni, O. Mattelaer, H.-S. Shao, T. Stelzer, et al., J. High Energy Phys. 1407 (2014) 079.
[33] G. Aad, et al., ATLAS Collaboration, Phys. Rev. D 91 (5) (2015) 052007, arXiv:1407.1376 [hep-ex].
[34] V. Khachatryan, et al., CMS Collaboration, Phys. Rev. D 91 (5) (2015) 052009, arXiv:1501.04198 [hep-ex].
[35] V. Khachatryan, et al., CMS Collaboration, Phys. Lett. B 740 (2015) 83, arXiv:1407.3476 [hep-ex].
[36] G. Aad, et al., ATLAS Collaboration, Phys. Lett. B 737 (2014) 223, arXiv:1406.4456 [hep-ex].
[37] G. Aad, et al., ATLAS Collaboration, Eur. Phys. J. C 75 (2) (2015) 69, arXiv:1409.6190 [hep-ex].
[38] G. Aad, et al., ATLAS Collaboration, Eur. Phys. J. C 75 (5) (2015) 209, arXiv:1503.04677 [hep-ex].
[39] V. Khachatryan, et al., CMS Collaboration, J. High Energy Phys. 1408 (2014) 174, arXiv:1405.3447 [hep-ex].
[40] V. Khachatryan, et al., CMS Collaboration, Phys. Rev. D 91 (9) (2015) 092005, arXiv:1408.2745 [hep-ex].
[41] G. Aad, et al., ATLAS Collaboration, J. High Energy Phys. 1409 (2014) 037, arXiv:1407.7494 [hep-ex].
[42] G. Aad, et al., ATLAS Collaboration, Phys. Rev. D 90 (5) (2014) 052005.
[43] V. Khachatryan, et al., CMS Collaboration, J. High Energy Phys. 1504 (2015) 025, arXiv:1412.6302 [hep-ex].
[44] G. Aad, et al., ATLAS Collaboration, Eur. Phys. J. C 75 (6) (2015) 263, arXiv:1503.08089 [hep-ex].
[45] V. Khachatryan, et al., CMS Collaboration, arXiv:1506.01443 [hep-ex].
[46] D. Stump, J. Huston, J. Pumplin, W.K. Tung, H.L. Lai, S. Kuhlmann, J.F. Owens, J. High Energy Phys. 0310 (2003) 046.
[47] T. Sjostrand, S. Mrenna, P.Z. Skands, J. High Energy Phys. 0605 (2006) 026;
T. Sjostrand, S. Mrenna, P.Z. Skands, Comput. Phys. Commun. 178 (2008) 852.
[48] Y.L. Dokshitzer, G.D. Leder, S. Moretti, B.R. Webber, J. High Energy Phys. 9708 (1997) 001.
[49] M. Wobisch, T. Wengler, *Hamburg 1998/1999, Monte Carlo generators for HERA physics*, pp. 270–279, arXiv:hep-ph/9907280.
[50] M. Cacciari, G.P. Salam, G. Soyez, Eur. Phys. J. C 72 (2012) 1896.
[51] The ATLAS Collaboration, ATLAS-PHYS-PUB-2014-004, http://atlas.web.cern.ch/Atlas/GROUPS/PHYSICS/PUBNOTES/ATL-PHYS-PUB-2014-004/.
[52] J.M. Butterworth, A.R. Davison, M. Rubin, G.P. Salam, Phys. Rev. Lett. 100 (2008) 242001.
[53] The ATLAS Collaboration, ATLAS-CONF-2013-086.
[54] M.E. Peskin, T. Takeuchi, Phys. Rev. Lett. 65 (1990) 964;
M.E. Peskin, T. Takeuchi, Phys. Rev. D 46 (1992) 381;
B. Holdom, J. Terning, Phys. Lett. B 247 (1990) 88;
M. Golden, L. Randall, Nucl. Phys. B 361 (1991) 3.
[55] K. Haba, S. Matsuzaki, K. Yamawaki, Phys. Rev. D 82 (2010) 055007.
[56] R. Casalbuoni, A. Deandrea, S. De Curtis, D. Dominici, F. Feruglio, R. Gatto, M. Grazzini, Phys. Lett. B 349 (1995) 533;
R. Casalbuoni, A. Deandrea, S. De Curtis, D. Dominici, F. Feruglio, R. Gatto, M. Grazzini, Phys. Rev. D 53 (1996) 5201.
[57] S. Matsuzaki, K. Yamawaki, in preparation.
[58] M. Bando, T. Fujiwara, K. Yamawaki, Prog. Theor. Phys. 79 (1988) 1140.